Transport and deposition of suspended particles in saturated porous media: hydrodynamic effect

Nasre-Dine Ahfir · Hua Qing Wang · Ahmed Benamar · Adbellah Alem · Nicolas Massei · Jean-Paul Dupont

Abstract A laboratory study was undertaken to determine the transport and deposition rate of suspended particles in columns of saturated porous media (gravel and glass beads), where the porous media were subjected to steady-state flow. Silt particles with a mode of 14 μm diameter (used as the suspended particles) and fluorescein (as the conservative tracer) were injected into the columns in short pulses. The breakthrough curves were competently described with the analytical solution of a convection–dispersion equation with a first-order deposition rate. The experiments were performed using different flow rates. The suspended particle size distribution, the porous media, and the flow rates themselves were the main factors retained in this study to investigate the mechanisms governing the transport and deposition kinetics in detail. The results showed the existence of a flow rate, beyond which suspended particles travel faster than the conservative tracer. A decrease of the deposition rate of suspended particles beyond a critical flow velocity was also observed. Such behaviour led to consideration of the couple hydrodynamic-gravity forces at high flow rates. As the hydrodynamic force increases, particle deposition rates are reduced due to the effect of hydrodynamic forces inhibiting the deposition.

Résumé Une étude expérimentale en colonne de laboratoire a été menée pour analyser le transport et la cinétique de dépôt des particules en suspension, en écoulement permanent, dans deux milieux poreux saturés (gravier et billes de verre). Des particules de limon d'un diamètre modal de 14 μm (utilisées comme particules en suspension) et de la fluorescéine (comme traceur conservatif) sont introduits dans la colonne par des injections impulsions. Les courbes de restitution sont bien décrites par la solution analytique de l'équation de convection dispersion avec une cinétique de dépôt de premier ordre. Les expériences sont réalisées avec différents débits d'écoulement. La distribution de taille des particules en suspension, le milieu poreux et la vitesse d'écoulement sont les facteurs principaux retenus dans cette étude pour analyser les mécanismes régissant le transport et la cinétique de dépôt. Les résultats ont montré l'existence d'un débit au-delà duquel les particules en suspension sont transportées plus rapidement que le traceur conservatif. La diminution de la cinétique de dépôt des particules en suspension au-delà d'une vitesse critique est aussi observée. Ce comportement est lié à la compétition entre les forces hydrodynamiques et de gravité à forts débits. La cinétique de dépôt des particules diminue à mesure que la force hydrodynamique augmente, empêchant le dépôt.

Resumen Un estudio del laboratorio fue emprendido, para determinar la tasa de transporte y depositación de partículas suspendidas, en unas columnas de medios porosos saturados (bolitas de grava y vidrio), dónde los medios porosos fueron sometidos a un flujo estacionario. Las partículas de limo con una moda de 14 μm de diámetro (usadas como las partículas suspendidas) y la fluoresceína (como el trazador conservador), se inyectaron en las columnas a manera de pulsos cortos. Las curvas de llegada se describieron adecuadamente con la solución analítica de una ecuación de dispersión-convección, con una tasa de depositación de primer orden. Los experimentos se realizaron usando diferentes tasas de flujo. La distribución de tamaño de las partículas suspendidas, el medio poroso, y las tasas de flujo en si mismas, fueron los factores principales contenidos en este estudio, para investigar los mecanismos que gobiernan el transporte y cinética de la depositación en detalle. Los resultados mostraron la existencia de una tasa de flujo, más allá de la cual, las partículas en suspensión, viajan más rápidamente que el trazador conservador. También fue observada una disminución de la tasa de la depositación de las partículas suspendidas más allá de una velocidad de flujo crítica. Tal comportamiento llevó a la consideración de la pareja de fuerzas hidrodinámica-gravedad en tasas de flujo altas. Con el aumento de la fuerza hidrodinámica, las tasas de

Received: 16 November 2005 / Accepted: 29 October 2006
Published online: 21 November 2006

N.-D. Ahfir (✉) · H. Q. Wang · A. Benamar · A. Alem
Laboratoire de Mécanique, Physique et Géosciences,
Université du Havre,
BP 540 Quai Frissard, 76058, Le Havre, France
e-mail: nasre-dine.ahfir@univ-lehavre.fr

N. Massei · J.-P. Dupont
UMR 6143 "M2C" CNRS/Université de Rouen,
76821, Mont-Saint Aignan Cedex, France

 DOI 10.1007/s10040-006-0131-3

depositación de partículas se reducen, debido al efecto de fuerzas hidrodinámicas que inhiben la depositación.

Keywords Tracer tests · Laboratory experiments/measurements · Hydrodynamic · Suspended particles · Deposition rate

Introduction

Particle transport in water is of interest to many applied disciplines. Among them are the industrial fields, which are concerned with various techniques for particle separation and filtration (e.g. chromatography, ultrafiltration, water treatment) and the Earth sciences where suspended particles play a major role, for example, in hydrogeology. Many investigations on colloid (≤1 µm) and microorganism transport, deposition and release mechanisms are available in the literature (Elimelech et al. 1995; Kretzschmar et al. 1997; Grolimund et al. 1998; Hater et al. 2000). Colloidal particles have been studied most often because of their abundance in groundwater and their physical properties such as specific surface area, large adsorption capacity, and low settlement rates (McDowell-Boyer et al. 1986). Owing to their larger size and density, suspended particle transport has only recently attracted significant attention (Frey et al. 1999; Gohr Pinheiro et al. 1999; Wang et al. 2000; Massei et al. 2002; Benamar et al. 2005). Various restrictions on the movement of suspended particles such as straining and filtration have been studied (McGechan and Lewis 2002). During the flow of the suspension through a medium, particle transport and capture are the result of several forces and mechanisms depending on particle density and size (Herzig et al. 1970). For large suspended particles (> 10 µm), hydrodynamics, gravity and inertial effects are dominant (Frey et al. 1999), while all forces and mechanisms can contribute to particle deposition for small suspended particles whose size is between 0.1 and 10 µm (Gohr Pinheiro et al. 1999). The boundary between colloidal and suspended particles is conventionally fixed at 1 µm. This boundary is rather arbitrary, but can be broadly justified for a number of reasons such as relative significant particle interactions (surface forces) and external forces such as those arising from gravitational and hydrodynamic effects (Elimelech et al. 1995). It follows that, as particle size decreases, colloid interactions become increasingly significant relative to external forces. Perturbations to groundwater chemical conditions, like a decrease in ionic strength accompanying the injection of recharge water to deep aquifers, mobilize existing particles by increasing the repulsive electrostatic forces between particles. Perturbations to groundwater physical conditions such as an increase in the groundwater velocity caused by pumping, mobilize existing particles through additional hydrodynamic shear (Ryan and Elimelech 1996).

Many studies in laboratory columns have been conducted recently in order to investigate the different parameters governing the transport of particles in homogeneous media (Wang et al. 2000), heterogeneous media (Delay et al. 1997) or fractured media (Toran and Palumbo 1992). Thus, using a laboratory column, one can control the fluid, the particle size distribution and the flow rate.

This paper presents a laboratory study devoted to the transport and deposition rate of the suspended particles within two highly permeable porous media under Darcy flow conditions. The materials used are crushed flint gravel and glass beads. The analytical solution of a convection–dispersion equation (CDE) with a first-order deposition rate describes the breakthrough of the suspended particles well. The objective of this study is to investigate the transport and deposition kinetics of suspended particles in water-saturated porous media under moderate and high flow rates.

Materials and methods

Spherical glass beads of 3 mm diameter (manufactured by Verre Industrie, France) and crushed silica gravel flint were used as the porous media in-filling the columns in the experiments. The gravel grain size distribution was 1.00–2.15 mm (20%) and 2.15–3.15 mm (80%; Fig. 1). To remove the impurities, the gravel material was washed in tap water until the rinse water was free of suspended impurities and then dried in an oven for 24 h at 105°C. The bulk density was obtained by weighing a known volume of the material; its value was 1.37 and 1.49 g/cm^3 for the gravel and glass beads, respectively. The specific density was obtained by adding demineralised water to a known mass of material until a fixed volume was obtained. The average value of specific density determined after three tests was 2.49 and 2.51 g/cm^3 for the gravel and glass beads, respectively. The total porosity of the porous medium was deduced as follows

$$\text{Total porosity} = 1 - \frac{\text{Bulk density}}{\text{Specific density}} \tag{1}$$

The resulting total porosity was 46% (±1%) for the gravel and 41% (±1%) for the glass beads. Measurements of hydraulic conductivity (K) of saturated porous media in

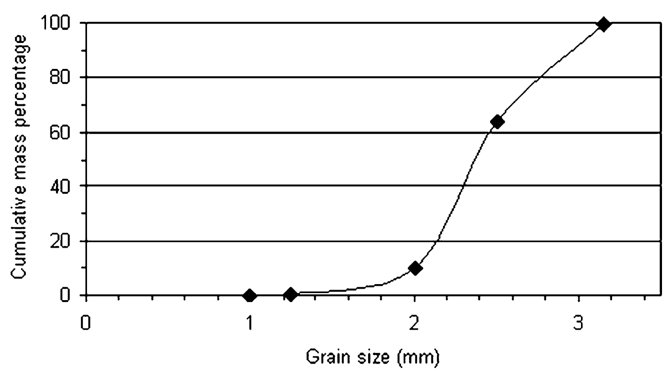

Fig. 1 Size distribution of the gravel filling one of the columns

DOI 10.1007/s10040-006-0131-3

the laboratory columns were based on the direct application of Darcy's law. For a constant head, the hydraulic gradient was held constant and the discharge through the porous medium was measured. The experiment was repeated for several gradients. The average hydraulic conductivity value of the gravel and glass beads was $K=2.26\times10^{-2}$ m/s and $K=2.12\times10^{-2}$ m/s, respectively.

The injected suspended particles consist of silt collected from Haute Normandie (France) surface formations. According to the microgranulometric spectrum (Fig. 2) that was acquired using a Coulter Multisizer particle counter (Coulter Electronics, counting by electrical impedance), the suspended particles ranged between 2 and 30 μm with a mode of 14 μm and a density close to 2.65 g/cm^3. Figure 3 presents a SEM (scanning electron microscopy) image of the population of silt particles from the Haute Normandie silt which mainly consist of quartz and are irregular in shape, both narrow and wide. A 500-ppb (parts per billion, i.e. 0.5 mg/l) solution of fluorescein (uranine), acting as the solute tracer, was used in order to compare solute transport behaviour with that of the silt particles. Although fluorescein is pH sensitive and degrades in strong light, it undergoes little to no interaction with inorganic materials and was thus assumed to act conservatively during the column tests (Porel 1988). Throughout this paper, "suspended particles" refers to the silt and "conservative tracer" refers to the fluorescein.

The column was packed in 5-cm increments by pouring the material (either glass beads or gravel) into the column, mixed with fresh water. Throughout filling, the column was subjected to vibrations that ensured even packing. Material mass in the column was measured in order to ensure the reproducibility of the experiments. The column was installed in a horizontal position for the tracer experiments in order to avoid an unequal packing down along the column, thus making the porous medium heterogeneous in its permeability. This phenomenon does not affect the columns of small dimensions, but could occur in this case because of the high flow rates tested and the amount of material packed within the column.

The experimental setup (Fig. 4) used a Plexiglas column of 355 mm length and 89 mm inner diameter. The column was fed by a reservoir containing water (pH

Fig. 3 SEM (scanning electron microscopy) image of silt particle population used as suspended particulate tracer

of 6.8±0.1) using a MasterFlex peristaltic pump (Cole-Parmer Instrument) which controlled the flow rate. A digital MacMillan numeric flow meter was installed at the column inlet to measure the flow rate. A syringe was used to perform pulse injections. The column was fitted with three piezometers (P1, P2, and P3), allowing for measurement of head variations along the length of the column during and after the suspended particle injection (and thereby indicating hydraulic conductivity variation owing to the particle deposition).

The detection systems were a Fisher Scientific turbidimeter and a Turner Designs 10-AU fluorometer. The turbidimeter consisted of a nephelometer, which determines the turbidity level by measuring the amount of light scattered at 90° by the suspended particles. The measurements are converted and displayed in Nephelometric Turbidity Units (NTU). The measurement range of the Fisher Scientific turbidimeter is from 0.1 to 1,000 NTU. The particle concentrations in the effluent were determined with the help of correlations made a priori between suspended particles concentrations in water and NTUs. The fluorometer measures fluorescein tracer concentrations of the effluent passing through a sample chamber which requires a Daylight White Mercury Vapour Lamp

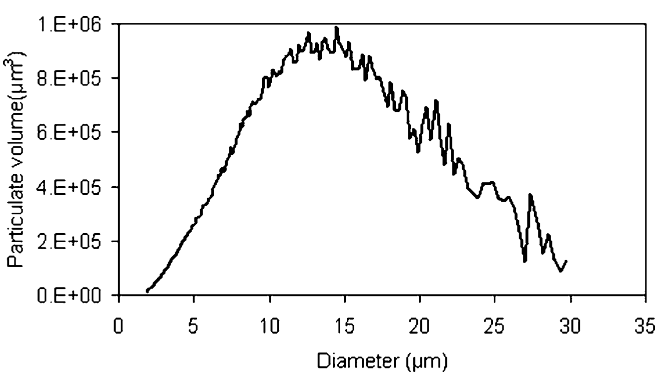

Fig. 2 Microgranulometric spectrum of the injected suspended particles (silt)

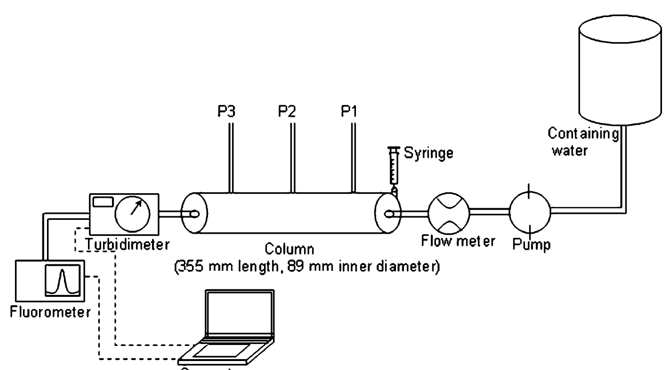

Fig. 4 Experimental set-up. Each column was equipped with three piezometers (*P1*, *P2* and *P3*)

DOI 10.1007/s10040-006-0131-3

F4T5 source, and an excitation (455–500 nm) and emission (510–700 nm) filter. The fluorometer is able to detect a fluorescein (excitation wavelength 490 nm, emission wavelength 512 nm) concentration of 0.1 ppb. The fluorometer was also calibrated to the fluorescein concentrations in water effluent.

For each porous medium column, three tracer test series were performed. After each experimental series, the material was washed to remove any suspended particles and dried at 105°C prior to being repacked within the column.

In each series, ten short pulse injections (each 20 ml) were performed. To compare suspended particles and conservative tracer (fluorescein) transport behaviour, each injected pulse consisted of a mixture of 0.1 g/l of suspended particles and 500 ppb of fluorescein. For each injection, the flow rate was kept constant (controlled by a peristaltic pump). The series of injections was performed starting from the highest flow rate (first injection) to the lowest one (last injection). This technique was chosen in order to avoid a likely release of the suspended particles previously deposited in the porous medium. Each injected pulse (20 ml) was small with respect to the column's pore volume (V_{p}) in order to avoid disturbing the water flow in the column (Kretzschmar et al. 1997). The ratio of the injected pulse to the glass beads or gravel pore volume was close to 2%. The tested flows varied from 1.630 to 0.050 l/min, corresponding to Darcy's velocities ranging from 0.4370 to 0.0134 cm/s. These values exceed natural flow velocities in aquifers, but are moderate for forced flows such as artificial recharge of aquifers. To illustrate the flow regime, Darcy's velocity (U) versus hydraulic gradient (i) was plotted (Fig. 5). A linear relationship is observed indicating that Darcy's law remains applicable in this investigation (laminar regime).

At each test, the duration of the injected pulse was sufficiently short to be considered instantaneous. For each suspended particles pulse injection, one sample (120 ml) was collected at the column outlet when the concentration reached the maximum value (breakthrough curve peak), for microgranulometric spectral analysis with a Coulter Multisizer Counter.

Owing to the high velocities tested (mean pore water velocities ranged from 0.950 to 0.030 cm/s), low ionic strength [2.6 mM (millimolar) NaCl], larger suspended particle size (a mode of 14 μm), and neutral water pH, chemical mechanisms were excluded from the assessment of processes involved in the study. Thus, the present study is restricted to physical (hydrodynamic) mechanisms involved in suspended particle transport and deposition.

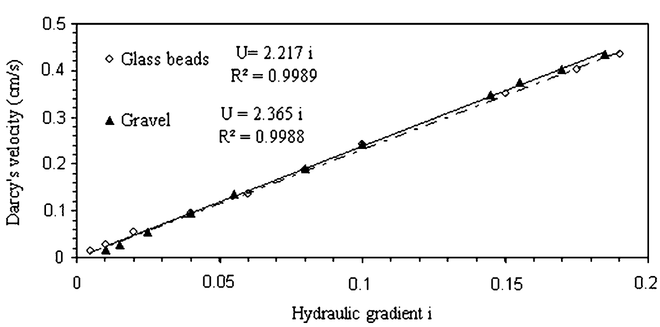

Fig. 5 Darcy's velocity as a function of hydraulic gradient

Mathematical modelling

Under steady-state and saturated flow conditions, the transport of particles through porous media can be described with a convection–dispersion equation (CDE) including a term for a first-order deposition rate (Kretzschmar et al. 1997; Grolimund et al. 1998):

$$\frac{\partial C}{\partial t} = D_{\mathrm{L}} \frac{\partial^2 C}{\partial x^2} - u \frac{\partial C}{\partial x} - K_{\mathrm{dep}} C \tag{2}$$

where C is the particle concentration in the solution (M/L^3), t is the time (T), x is the travel distance (L), D_{L} is the longitudinal dispersion coefficient (L^2/T), u is the average pore water velocity (L/T), and K_{dep} is the deposition rate coefficient (T^{-1}). In this equation, particle release is neglected. Equation (2) assumes that particle deposition follows first-order kinetics and is irreversible. This assumption is justified at sufficiently low particle concentration (i.e. no blocking or ripening effect; Elimelech et al. 1995; Kretzschmar et al. 1997). A short pulse is mathematically considered as an instantaneous injection. The initial and boundary conditions for a semi-infinite medium are given by Eq. (3).

$$\left.\begin{array}{l} C(t=0,x)=0 \\ C(t,x=0)=m/Q\delta(t) \\ C(t,x=\infty)=0 \end{array}\right\} \tag{3}$$

Where $\delta(t)$ is the Dirac delta function, m is the mass of particles injected (M), and Q is the flow rate (L^3/T). The last boundary condition [$C(t,x=\infty)=0$] is not realistic for limited column length, but necessary for providing an analytical solution. The analytical solution for Eq. (2), according to Eq. (3), is given as follows (Wang et al. 2000):

$$C(t,x) = \frac{mx}{Q\sqrt{4\pi D_{\mathrm{L}} t^3}} \exp\left(-K_{\mathrm{dep}} t\right) \exp\left[-\frac{(x-ut)^2}{4D_{\mathrm{L}} t}\right] \tag{4}$$

Based on the analytical solution (Eq. 4), the regression parabolic method (Wang 2001) is used in order to interpret the breakthrough data. Regression parabolic method (RPM) is a derivative as an extension of the linear graphical method (Wang et al. 1987) to deal with problems involving three parameters. For the tracer tests, this method allows immediate determination of the dispersion coefficient (D_{L}), the convection time ($t_{\mathrm{c}} = L/u$, where L is the column length) and the deposition rate

 DOI 10.1007/s10040-006-0131-3

coefficient (K_{dep}). The recovery rate (R) is also estimated by integrating the experimental breakthrough curves (BTCs). In the case of dissolved conservative tracer (fluorescein), no deposition occurs. Thus, only two parameters were determined (D_L and t_c).

Results and discussion

The transport experiments have been interpreted by the mathematical model presented above. The BTCs were fitted with the analytical solution, Eq. (4), and the transport parameters were determined. Figure 6 shows comparisons between experimental data and those computed according to the regression parabolic method (RPM). Note that, the relative concentration C_R is derived from the above method and expressed, for both particles and tracer, as:

$$C_R = \frac{CV_P}{m} = \frac{CV_P}{V_{inj}C_O} \quad (5)$$

where V_p is the pore volume of the porous medium (L^3), and V_{inj} is the volume of each injection (L^3), and C_0 is the initial concentration (M/L^3). By adjustment, a good fit of the experimental BTCs with those calculated by the model is obtained for all flow velocities tested (Fig. 6), and for both suspended particles (SP) and conservative tracer. The experimental results are represented well by the mathematical model.

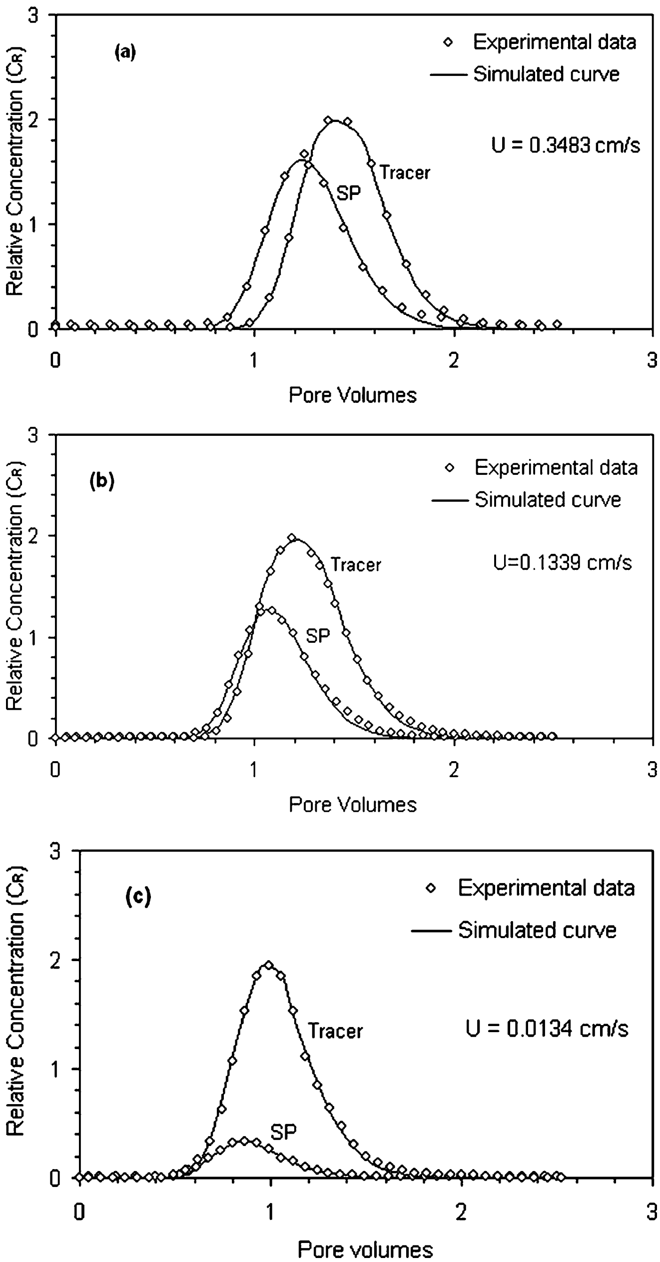

Fig. 6 Fitting of the experimental breakthrough curves (BTCs) of silt suspended particles (*SP*) and conservative tracer (fluorescein) with the mathematical model, for **a** high, **b** medium and **c** low Darcy's velocity (U)

Influence of flow velocity on the dispersivity

The longitudinal dispersion coefficient (D_L) in Eq. (2) is a simplification for hydrodynamic dispersion, including the processes of mechanical dispersion and molecular diffusion. The mechanical dispersion is caused by a variation in fluid velocity in the pore space of porous media and the diffusion is caused by the random motion of molecules. However, these experiments conform to regime III ($300<Pe<10^5$) defined by Pfannkuch (1963) for the conservative tracer, i.e. mechanical dispersion dominates molecular diffusion, and where Pe is the Peclet number. Thus, the molecular diffusion is negligible. Assuming $D_L=\alpha_L u$, the longitudinal dispersivity α_L was calculated for both gravel and glass beads at the different flow rates tested in this study for the conservative tracer and the suspended particle tests. The longitudinal dispersion D_L was determined by fitting the breakthrough curves using Eq. (4). Figure 7 describes the variation of the suspended particles and the conservative tracer dispersivities as a function of Darcy's velocity. The obtained dispersivities of the conservative tracer from both the gravel and glass-beads columns range between 0.29 and 0.65 cm. The dispersivity of the conservative tracer in the glass-beads medium is of the order of glass bead size (0.34 cm) at high flows and twice its size at low flows (0.56 cm). For the gravel medium, dispersivity value varies from 1.5 to 2.5 times the mean grain size (d_{50}) at high and low flows, respectively. The dispersivity decreases with increasing flow velocity, i.e. the dispersivity increases when the convection time of the tracer increases within the porous medium. Dieulin (1980) reported the results of a dissolved tracer test conducted in a heterogeneous alluvial aquifer and concluded that the dispersivity increased with time.

The dispersivity values obtained from the gravel column are similar to those of the glass-beads column. The results further demonstrate that the conservative tracer dispersivity is smaller than that of the suspended particles (silt) over all velocities investigated (Fig. 6). This behaviour can be explained by the large size distribution

 DOI 10.1007/s10040-006-0131-3

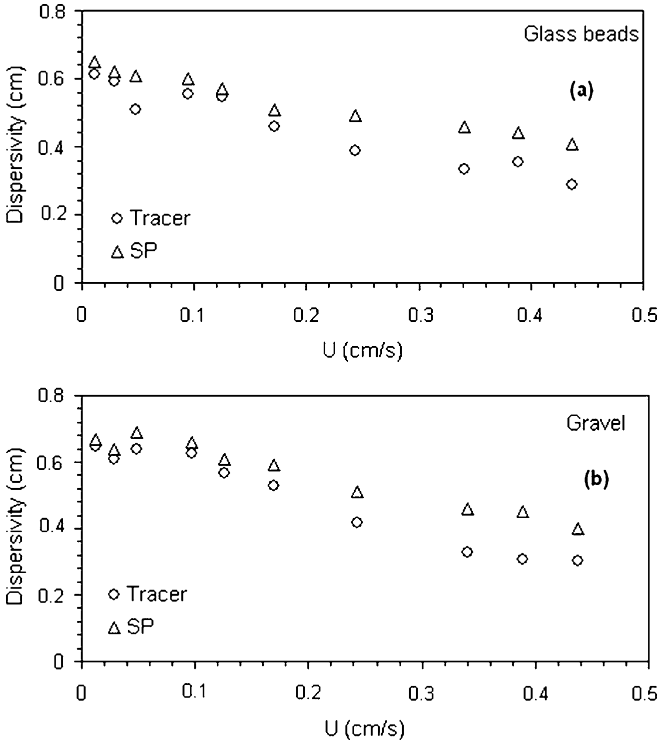

Fig. 7 Longitudinal dispersivity of tracer and suspended particles (*SP*) as a function of Darcy's velocity (*U*) for **a** glass beads and **b** gravel columns

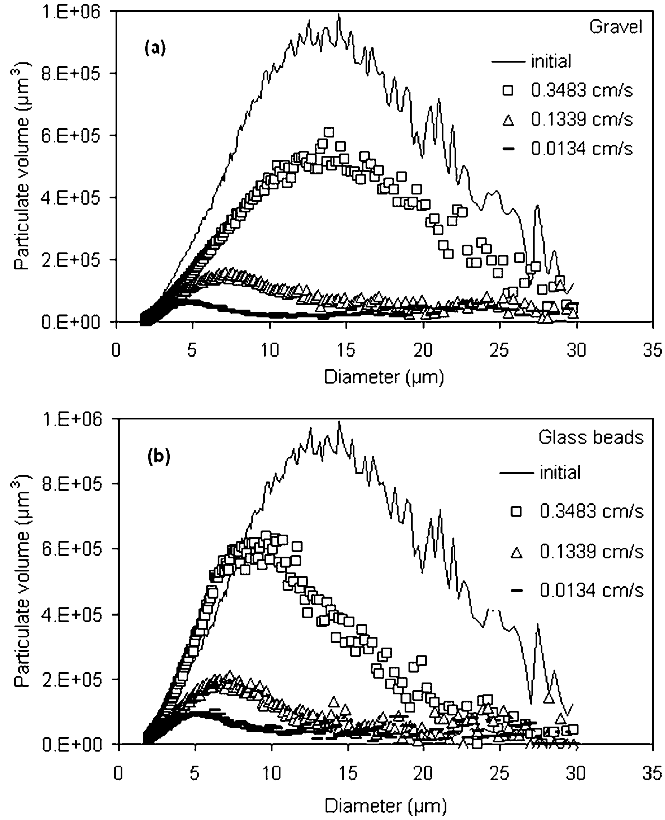

Fig. 8 Characterisation of the microgranulometric fractions of the suspended particles travelling through **a** gravel and **b** glass beads with subsequent high, medium and low Darcy's velocities. The initial injected suspended particles spectrum is represented by a *solid line*

of the suspended particles (Fig. 7, curve noted 'initial') which leads to a large dispersion of the particle velocities. This difference is more important at high flow rates where the size exclusion effect is more significant, as will be discussed in the next subsection dealing with the comparison between the suspended particle and the conservative tracer behaviour.

Particle size distribution during breakthrough

Suspended-particle size distribution is measured at the column outlet for each experiment at about the peak of the BTCs (Fig. 8). It is shown that for the high flow rates (e.g. 0.3483 cm/s), the recovery of coarser particles is more important in the gravel than in the glass-beads column. For example, at the velocity of 0.3483 cm/s, the diameter mode of the recovered particles is 14 µm for the gravel and only 8 µm for the glass beads. This can be explained by the existence of macropores in the gravel medium leading to easy travelling of the large suspended particles. The modal size of the recovered particles increases with flow rate. At low velocities, the recovered particles are mainly the smaller ones, because the hydrodynamic force exerted by the flow on the particles is insufficient to mobilise the larger particles, which remains trapped. Figure 9 presents the recovery rate, *R* (%), of the suspended particles at the column outlet for both glass beads and gravel columns. *R* is obtained by integrating the experimental breakthrough curves area. As emphasized above, the recovery rate increases with the flow rate. At a given flow velocity the particle recovery from the glass-beads column is larger than that from the gravel column, although the total porosity is more important in the gravel than in the glass beads (Fig. 9). This leads to consideration of the geometry of the pores and their distribution in the porous medium. In the gravel column, there are narrow and wide grain sizes, leading to a large pore distribution and then many retention sites such as constriction, crevice, and cavern sites participate in particle trapping. On the other hand, the single-size of the glass beads led to a quite uniform pore distribution; thus, one presumes that the pore

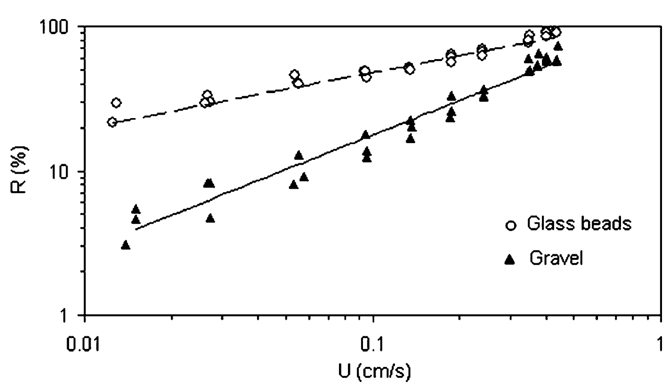

Fig. 9 Fraction of particles (*R*) recovered at the column outlet as a function of Darcy's velocity (*U*)

 DOI 10.1007/s10040-006-0131-3

constrictions are of the same dimension and contain only a few unconnected pores (dead-end-pore), giving rise to a better recovery rate.

Transport behaviour

This section discusses the comparison between the transport behaviour of the suspended particles and the conservative tracer. Tests carried out in the gravel and glass-beads columns reveal two features. First, breakthrough of the suspended particles (silt) occurred earlier than the conservative tracer at high flow velocities (Fig. 10a and c). The fast transport of the suspended particles compared to the conservative tracer is attributed to the size exclusion (Grolimund et al. 1998; Kretzschmar et al. 1997) where the suspended particles are transported in preferential pathways. In contrast to the conservative tracer, a portion of the pore space of the porous medium is not accessible to the suspended particles. Santos and Berdrikovtsky (2004) developed a population balance model for particulate suspension transport with size exclusion of particles by the porous media. Their model accounts for particle flux reduction and pore space accessibility due to the restriction on larger particles moving through smaller pores. According to their results, the larger the particle, the larger is its velocity. The large particles are the first to appear at the column outlet.

The fast transport of the suspended particles is also due to the velocity distribution in a pore. This effect was highlighted by Dodds (1982) in a chromatographic tube and named "hydrodynamic chromatography". Within a cylinder tube, and in a laminar flow regime, the microscopic velocity profile is parabolic, with the maximum velocity at the axis of the tube. Due to the transversal molecular diffusion, dissolved tracer is transported by all existing velocities in the tube. Thus, it is transported equally across the total section of the tube. Due to the size of the particles, Dodds (1982) observed that the larger particles can not be transported close to the wall because of their dimension. Thus, they are only transported by higher velocities near the tube axis, whereas the solute can approach the wall (lower velocities).

Second, below a certain flow rate, breakthrough of the conservative tracer occurred earlier than that of the

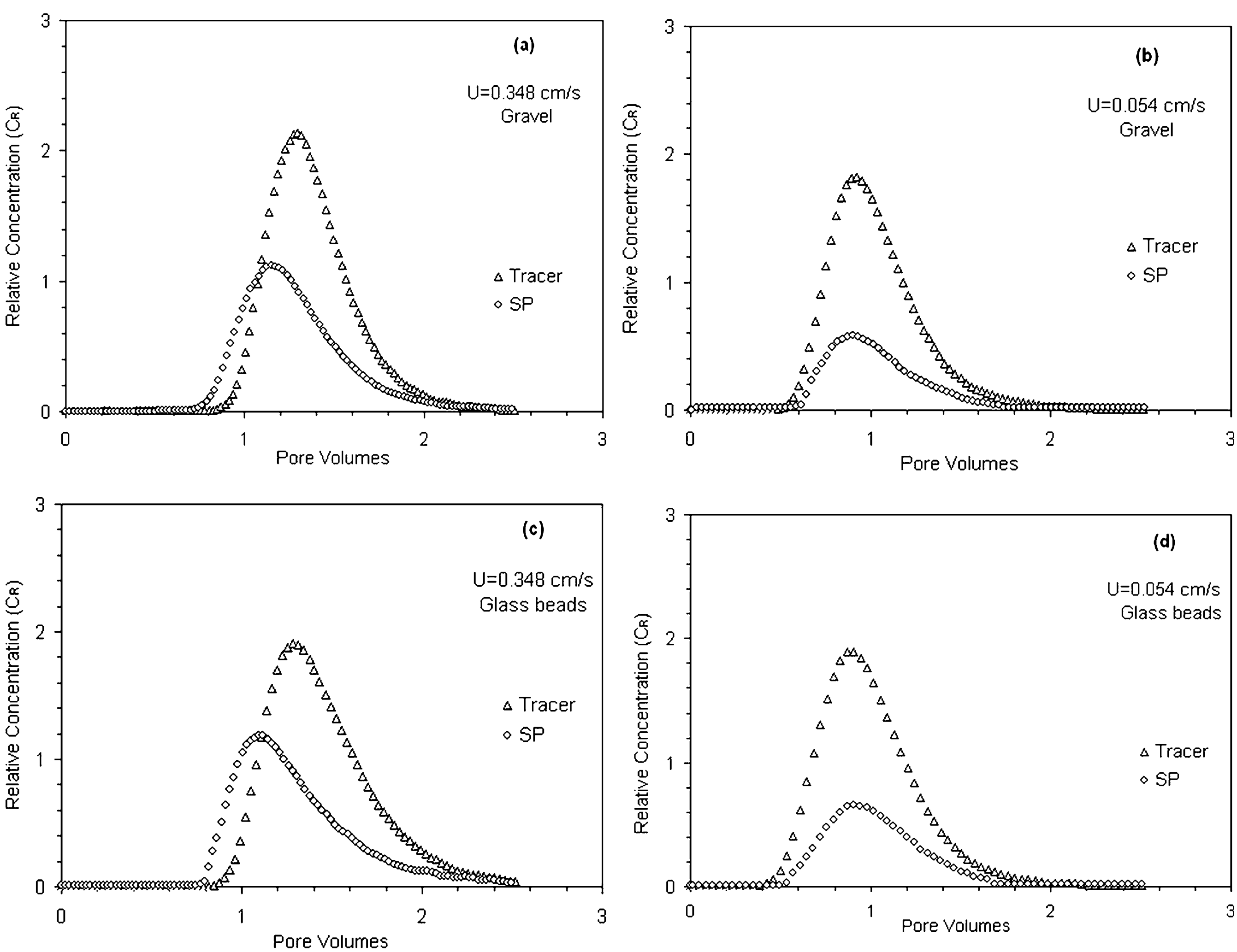

Fig. 10 Experimental breakthrough curves for the conservative tracer and suspended particles (*SP*) in the gravel column at **a** high and **b** low Darcy's velocity and in the glass-beads column at **c** high and **d** low velocity

 DOI 10.1007/s10040-006-0131-3

suspended particles which arrived at the column outlet (Fig. 10b and d). This behaviour can be explained by analysing the granular size distribution of the effluent (Fig. 8). As emphasized in the last section, the micro-granulometric spectrum mode decreases with decreasing flow rate. So, lower flow rate favoured transport of smaller suspended particles. Since dispersion might be more important for the transport of smaller suspended particles, compared to the conservative tracer, a similar or little retardation of the peaking of the suspended particles concentration was observed (Fig. 10b and d). Thus, at lower flow rates, the transport paths of smaller suspended particles were longer because of the detours in the porous medium before reaching the outlet. In other words, the arrival time (necessary time for the first suspended particles/tracer molecules to reach the exit of the column) of the suspended particles is greater in comparison with that of the conservative tracer. In contrast, a higher flow rate facilitated mobilisation of the larger suspended particles, but with a significant size exclusion that caused the preferential transport. At a lower flow rate, the larger suspended-particles entrapment within the porous media is due to settlement in narrower pores.

To quantify the shift of the initial breakthrough of the particles compared to the conservative tracer, a relative velocity factor, noted V_r, was defined as the ratio $(V_{SP}-V_T)/\ V_T$ where V_{SP} and V_T are the velocity of suspended particles and the conservative tracer respectively. Figure 11 shows the variation of the relative velocity as a function of Darcy's velocity. The earlier breakthrough of suspended particles is thus described by the positive values of V_r. The earlier breakthrough (V_r positive) of the suspended particles occurred at a lower velocity in the glass beads than in the gravel columns, i.e. 0.135 and 0.16 cm/s respectively. The transport behaviour difference between gravel and glass-beads media is mainly due to the porosity (pore-water velocity), the pore geometry and pore distribution. So, as emphasised in the last section, the gravel grain size distribution favours the trapping of suspended particles. Indeed, the suspended particle transport in glass-beads medium was facilitated by a homogeneous pore distribution.

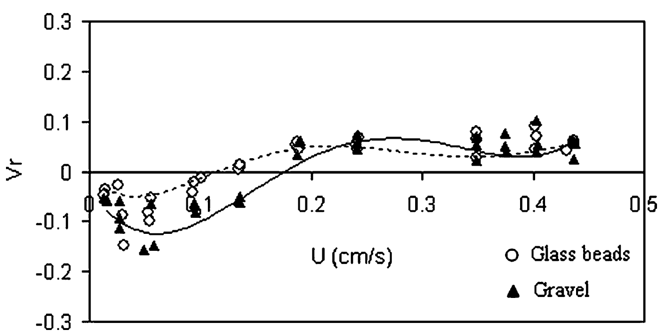

Fig. 11 Relative velocity factor of the suspended particles with respect to the conservative tracer (Vr) versus Darcy's velocity (U)

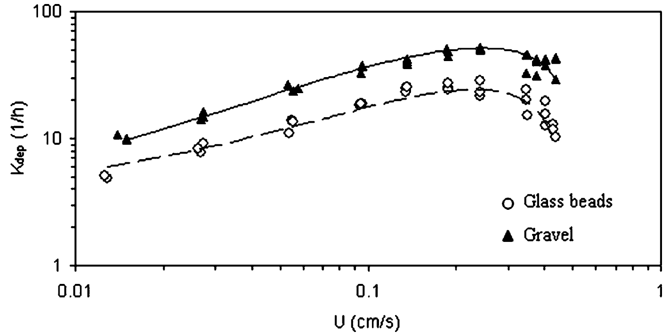

Fig. 12 Influence of flow velocity on deposition kinetics of silt particles as a function of water flow velocity (U). K_{dep} is the deposition rate coefficient

Influence of flow velocity on the deposition kinetics

The particle deposition rate as a function of flow velocity for glass beads and gravel columns is depicted in Fig. 12. The results show that deposition rate is more important in the gravel medium over all the flow rates tested. The heterogeneous pore distribution in the gravel favours particle deposition. The particle deposition rate increases with flow rate until a critical velocity, beyond which it decreases. Usually, the deposition rate is described by a power law ($K_{dep} \alpha U^n$). Massei et al. (2002) found a power value (n) of 0.7 for silt particles. Kretzschmar et al. (1997) found a power value of 0.31 for carboxyl latex colloids and 0.18 for humic-coated hematite colloids. In the present study, and below the critical velocity, the deposition rate is well described by a power law with values of 0.67 and 0.62 within the gravel and glass-beads columns, respectively. For particles smaller than about 1 μm, where diffusion dominates particle transport, Song and Elimelech (1993) predicted slope to the power of one-third, i.e. $K_{dep} \alpha U^{1/3}$ for deposition onto impermeable solid surfaces such as spherical collector grains. Song and Elimelech (1995) extended this analysis to particle deposition onto permeable surfaces, which allow the

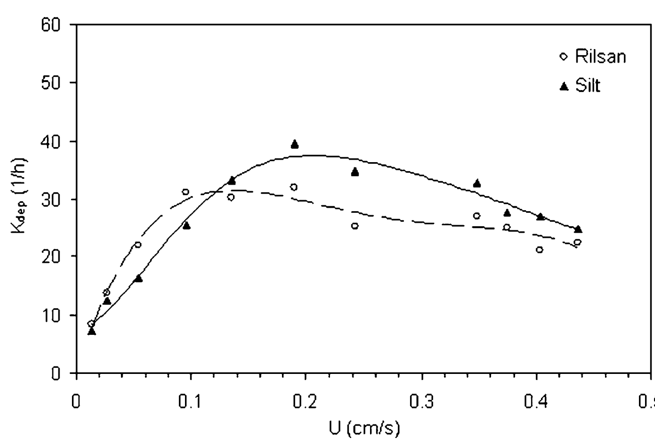

Fig. 13 Comparison of deposition rates of two types of suspended particles, silt and Rilsan, in a gravel column (adapted from Benamar et al. 2005)

 DOI 10.1007/s10040-006-0131-3

passage of fluid molecules through the pores but block the transport of colloidal particles. The deposition rate is controlled by the convection particle transport ($K_{dep} \alpha U$). In the present study, and in the tests conducted below the critical velocity, the dependence of the measured deposition rate coefficient on water velocity ($U^{0.62}$, $U^{0.67}$) is between what is expected for deposition onto impermeable surfaces ($U^{1/3}$) and permeable porous surfaces ($U^{1.0}$).

Although the laminar flow regime and Darcy's law remain applicable (Fig. 5), this does not discard the existence, at high velocities, of shear flow which is able to tear off particles leading to a decrease in deposition rate. At low flow rates, the deposition of larger suspended particles is mainly controlled by sedimentation, where the suspended particles were subjected to gravity and their velocity is no greater than the fluid velocity. Other capture mechanisms such as capture in constrictions and cavern sites occur too. As shown in Fig. 8, at low velocity, a mainly small suspended-particle population was recovered and the larger one was captured in the medium. Once the flow velocity rises, the hydrodynamic forces, especially drag force, are important. Then, the relative significance of sedimentation with respect to bulk flow is weak. Thus, the decreases in deposition can be explained by the fact that the hydrodynamic forces are significant and dominate the gravitational forces applied on the particles.

To assess the influence of suspended particle density on the deposition rate, Benamar et al. (2005) compared the deposition rate of the silt particles with that of Rilsan particles within a column packed with gravel. Rilsan particles (polyamide-11), manufactured by ATOFINA (France), have a size distribution ranging mainly from 15 to 35 μm with a mode of 25 μm. The density of the Rilsan particles is 1.04 g/cm^3, closer to that of water. The deposition rate versus Darcy's velocity of the silt and Rilsan particles is shown on Fig. 13. As for the silt particles, the deposition rate of the Rilsan particles increases with the flow rate until a critical velocity is reached and then decreases. Deposition rate decreases earlier for the Rilsan than for the silt particles. This is a consequence of the density of Rilsan which is close to that of water (1.04 g/cm^3) leading to insignificant sedimentation. On other hand, the gravity effect is more significant for silt owing to its density (2.65 g/cm^3). Although the size of the Rilsan particles is larger than that of the silt particles, it is enough for a small hydrodynamic force to prevent the Rilsan particle deposition. Thus, the deposition rate decreases early. While, for the silt particles, more important hydrodynamic force is needed to dominate the gravity effects for the larger suspended particles, thus the deposition rate decreasing occurs later. Yiantsios and Karabelas (1997, 2003) observed that if gravity forces are present (in a horizontal channel) they control deposition at low shear stress. As the hydrodynamic wall shear stress increases, particle deposition rates are significantly reduced due to the effect of hydrodynamic lift or drag forces inhibiting the deposition. According to these results, one can deduce that strong hydrodynamic forces play the double role of enhancing transport rates (Fig. 9), and reducing the particle deposition kinetics.

Conclusion

This study, devoted to transport and deposition of suspended particles in saturated media, showed that a one-dimensional convection–dispersion model with first-order deposition can successfully describe how the breakthrough curve and hydrodispersive parameters are derived. The conservative tracer dispersivity is smaller than that of the suspended particles as a result of the large size distribution of the suspended particles (polydispersive). The recovery rate increases with flow rate. The amounts of suspended particles recovered from the glass-beads column are greater than those from the gravel column. The larger suspended particles were most recovered at high velocity in the gravel compared with the glass-beads column. A size exclusion effect is observed at high flow rates leading to rapid transport of suspended particles with respect to the conservative tracer. The deposition rate increases with flow rate until a critical velocity beyond which it decreases. This behaviour is attributed to the fact that the hydrodynamic forces applied on the suspended particles at high flow rates dominate the gravitational forces, leading to reduce suspended particle deposition kinetics.

Acknowledgements The research is supported by "Région Haute Normandie". Irène Zimmerlin is gratefully acknowledged for her assistance in acquiring SEM images at the Laboratoire de Geologie (UMR 6143 M2C, Université de Rouen, France).

References

Benamar A, Wang HQ, Ahfir ND, Alem A, Massei N, Dupont JP (2005) Inertial effects on the transport and the rate deposition of fine particles in a soil. CR Geosci 337:497–504

Delay F, Porel G, de Marsily G (1997) Predicting solute transport in heterogeneous media from results obtained in homogeneous ones: an experimental approach. J Cont Hydrol 25:63–84

Dieulin A (1980) Propagation de pollution dans un aquifère alluvial: l'effet de parcours [Pollution propagation in an alluvial aquifer: path effect]. PhD Thesis, Université Paris-6, France

Dodds J (1982) La chromatographie hydrodynamique [Hydrodynamic chromatography]. Analusis 10:109–119

Elimelech M, Gregory J, Jia X, Williams RA (1995) Particle deposition and aggregation: measurement, modeling, and simulation. Butterworth-Heinemann, Oxford

Frey JM, Schmitz P, Dufreche I, Gohr Pinheiro I (1999) Particle deposition in porous media: analysis of hydrodynamic and weak inertial effects. Transp Porous Media 37:25–54

Gohr Pinheiro I, Schmitz P, Houi D (1999) Particle capture in porous media when physico–chemical effects dominate. Chem Eng Sci 54:3801–3813

Grolimund D, Elimelich M, Borcovec M, Barmettler K, Kretzschmar R, Sticher H (1998) Transport of in situ mobilized colloidal particles in packed soil columns. Environ Sci Technol 32: 3562–3569

Hater T, Wagner S, Atwill ER (2000) Colloid transport and filtration of cryptosporidium parvum in sandy soils and aquifer sediments. Environ Sci Technol 34:62–70

 DOI 10.1007/s10040-006-0131-3

Herzig JP, Leclerc DM, Le Goff P (1970) Flow of suspension through porous media: application to deep bed filtration. Ind Eng Chem 62:8–35

Kretzschmar R, Barmettler K, Grolimund D, Yan YD, Borkovec M, Sticher H (1997) Experimental determination of colloid deposition rates and collision efficiencies in natural porous media. Water Resour Res 33:1129–1137

Massei N, Lacroix M, Wang HQ, Dupont JP (2002) Transport of particulate material and dissolved tracer in a highly permeable porous medium: comparison of the transfer parameters. J Contam Hydrol 57:21–39

McDowell-Boyer LM, Hunt JR, Sitar N (1986) Particle transport through porous media. Water Resour Res 22:1901–1921

McGechan MB, Lewis DR (2002) Transport of particulate and colloid-sorbed contaminants through soil, Part 1: general principales. Biosystems Eng 83:255–273

Pfannkuch HO (1963) Contribution à l'étude des déplacements de fluides miscibles dans un milieu poreux [Contribution to the study of miscible fluids displacements in a porous medium]. Rev Inst Fr Pétrol 18:215–270

Porel G (1988) Transfert de soluté en aquifère crayeux: Causes de modifications des résultats de traçages [Solute transport in chalk aquifer: causes of tracer modifications results]. PhD Thesis, Lille University, France

Ryan JN, Elimelech M (1996) Colloid mobilization and transport in groundwater. Colloids Surf A Physicochem Eng Asp 107:1–56

Santos A, Berdrikovtsky P (2004) Size exclusion during particle suspension transport in porous media: stochastic and averaged equations. CAM 23:259–284

Song L, Elimelech M (1993) Calculation of particle deposition rate under unfavorable particle-surface interactions. J Chem Soc Trans 89:3443–3452

Song L, Elimelech M (1995) Particle deposition onto a permeable surface in laminar flow. J Colloid Interface Sci 173: 165–180

Toran L, Palumbo AV (1992) Colloid transport through fractured and unfractured laboratory sand columns. J Cont Hydrol 9: 289–303

Wang HQ (2001) Transferts de matières en milieu saturé: outils mathématiques et modélisation numérique [Mass transfer in saturated porous media: mathematical tools and numerical modelling]. Mémoire HDR, Université de Rouen, France

Wang HQ, Crampon N, Huberson S, Garnier JM (1987) Linear graphical method for determining Hydrodispersive characteristics in tracer experiments with instantaneous injection. J Hydrol 95:143–154

Wang HQ, Lacroix M, Massei N, Dupont JP (2000) Particle transport in porous medium: determination of hydrodispersive characteristics and deposition rates. CR Acad Sci Paris Sci Terre Planèt 331:97–104

Yiantsios SG, Karabelas AJ (1997) The effect of gravity on deposition of micron-sized particles on smooth surfaces. Int J Multiphase Flow 24:283–293

Yiantsios SG, Karabelas AJ (2003) Deposition of micron-sized particles on flat surfaces: effects of hydrodynamic and physicochemical conditions on particle attachment efficiency. Chem Eng Sci 58:3105–3113

 DOI 10.1007/s10040-006-0131-3